

Luminescent Lanthanide Metal-Organic Frameworks with a Large SHG Response

Song Dang,^a Jian-Han Zhang^b, Zhong-Ming Sun^{*a,b} and Hongjie Zhang^a

^a State Key Laboratory of Rare Earth Resource Utilization, Changchun Institute of Applied Chemistry, Chinese Academy of Sciences, 5625 Renmin Street, Changchun, Jilin 130022, P.R. China.

^b State Key Laboratory of Structural Chemistry, Fujian Institute of Research on the Structure of Matter, Chinese Academy of Sciences, Fuzhou 350002, P.R. China.

Table of Contents

1. Materials and Synthesis.....	S2
2. Instrumentation.....	S2
3. X-ray crystal structure determination.....	S3
4. Crystal data for LnL	S3
5. PXRD Analysis.....	S7
6. Luminescence measurements.....	S8
7. Diffuse reflectionspectra.....	S10
8. Thermogravimetric Analysis.....	S10
9. NLO measurements.....	S11
References.....	S12

1. Materials and Synthesis

All reagents were purchased commercially and used without further purification.

Typical synthesis of LnL: The ligand H_6L was synthesized according to the literature record.^[1] Taking **LaL** as an example, H_6L (0.1mmol, 86.6mg), $La(NO_3)_3 \cdot 6H_2O$ (0.1mmol, 43mg), DMF (7 ml), H_2O (1 ml) and diluted nitric acid (1 M, 1 ml) were placed in a 20 ml Teflon-lined stainless steel autoclave, which was kept at 160 °C for 3 days, and then cooled to room-temperature. After washed by water and ethanol, the colorless crystals were obtained, yield 52.18 mg (75 %, based on La ion). Elemental analysis (%) calcd for **LaL**: C, 49.97 %; H, 3.88 %; N, 2.01 %. Found: C, 50.07 %; H, 3.97 %; N, 1.92 %. Other crystals were synthesized similar to **LaL** using compounds $Ln(NO_3)_3 \cdot 6H_2O$. Elemental analysis (%) calcd for **EuL**: C, 49.05 %; H, 3.81 %; N, 1.97 %. Found: C, 49.21 %; H, 3.96 %; N, 1.88 %. Elemental analysis (%) calcd for **TbL**: C, 48.57 %; H, 3.77 %; N, 1.95 %. Found: C, 48.64 %; H, 3.86 %; N, 1.84 %.

Synthesis of $Eu_{0.05}La_{0.95}L$ and $Tb_{0.08}La_{0.92}L$: Similar synthesis processes were employed to synthesize $Eu_{0.05}La_{0.95}L$ and $Tb_{0.02}La_{0.98}L$ by adding a different amount of lanthanide ions of $Eu(NO_3)_3 \cdot 6H_2O$, $Tb(NO_3)_3 \cdot 6H_2O$, and $La(NO_3)_3 \cdot 6H_2O$. Elemental analysis (%) calcd for **$Eu_{0.05}La_{0.95}L$** : C, 49.92 %; H, 3.87 %; N, 2.01 %, Eu, 1.09 %. Found: C, 50.01 %; H, 3.99 %; N, 1.98 %, Eu, 1.15 %. Elemental analysis (%) calcd for **$Tb_{0.08}La_{0.92}L$** : C, 49.85 %; H, 3.86 %; N, 2.02 %, Tb, 1.82 %. Found: C, 49.94 %; H, 3.77 %; N, 2.04 %, Tb, 1.91 %.

2. Instrumentation

The elemental analyses of C, H, N, and Ln ions in the solid samples were carried out on a VarioEL analyzer (Elementar Analysensysteme GmbH) and via inductively coupled plasma (ICP) atomic emission spectrometric analysis (POEMS, TJA), respectively. Thermogravimetric analysis (TGA) was made using a SDT 2960 Simultaneous DSC-TGA of TA instruments up to 800 °C, and the heating rate was 10 °C min⁻¹ under an air flow of 100 mL min⁻¹. Powder X-ray power diffraction (XRD)

patterns were performed on a D8 Focus (Bruker) diffractometer with Cu K α radiation Field-emission ($\lambda = 0.15405$ nm, continuous, 40 kV, 40 mA, increment = 0.02°). The measurement of the powder frequency-doubling effect was carried out by means of the method of Kurtz and Perry. The fundamental wavelength is 1064 nm generated by a Q-switched Nd: YAG laser. The SHG wavelength is 532 nm. KH₂PO₄ (KDP) was used as reference to assume the effect. The luminescence spectra were recorded on a Hitachi F-4500 fluorescence spectrophotometer. The photomultiplier tube (PMT) voltage was 700V, the scan speed was 1200 nm·min⁻¹, the slit width of excitation and emission is 2.5 nm.

3. X-ray crystal structure determination

Suitable crystals with dimensions of $0.14 \times 0.12 \times 0.10$ mm³, $0.13 \times 0.11 \times 0.10$ mm³ and $0.14 \times 0.12 \times 0.11$ mm³ for **LaL**, **EuL** and **TbL** compounds, respectively, were selected for single crystal X-ray diffraction analysis. Crystallographic data were collected at 273 K on a Bruker Apex II CCD diffractometer with graphite monochromated Mo-K α radiation ($\lambda = 0.71073$ Å). Data processing was accomplished with the SAINT program. The structure was solved by direct methods and refined on F^2 by full-matrix least squares using SHELXTL-97. Non-hydrogen atoms were refined with anisotropic displacement parameters during the final cycles. All hydrogen atoms of the organic molecule were placed by geometrical considerations and were added to the structure factor calculation. Isolated solvents within the channels were not crystallographically well-defined. The DMF molecules were determined on the basis of crystal data, TGA and elemental microanalysis.

4. Crystal data for LnL (Ln = La, Eu, and Tb)

Table S1. Crystallographic data and structure refinement for **LnL** (Ln = La, Eu, Tb).

Compound	LaL	EuL	TbL
CCDC	891416	891417	891418
Empirical formula	C ₂₉ H ₂₇ NO _{10.5} La	C ₂₉ H ₂₇ NO _{10.5} Eu	C ₂₉ H ₂₇ NO _{10.5} Tb

F_w	696.43	709.48	716.44
Crystal system	Monoclinic	Monoclinic	Monoclinic
Space group	C2	C2	C2
$a/\text{Å}$	33.136(6)	32.789(3)	32.6663(15)
$b/\text{Å}$	7.3933(12)	7.1091(7)	7.0665(3)
$c/\text{Å}$	14.349(2)	14.5399(15)	14.5262(7)
α°	90	90	90
β°	104.510(3)	104.454(2)	104.3980(10)
γ°	90	90	90
$V/\text{Å}^3$	3403.2(10)	3281.9(6)	3247.9(3)
Z	4	4	4
T, K		273(2)	
λ (Mo K α), Å		0.71073	
F(000)	1396	1420	1428
Crystal size(mm ³)	0.14 × 0.12 × 0.10	0.13 × 0.11 × 0.10	0.14 × 0.12 × 0.11
ρ_{calcd} (g cm ⁻³)	1.467	1.436	1.465
μ (Mo K α), mm ⁻¹	1.306	1.964	2.231
R_1/wR_2 ($I > 2\sigma(I)$) ^a	0.0460/0.1185	0.0384/0.0894	0.0354/0.0905
R_1/wR_2 (all data)	0.0588/0.1320	0.0465/0.0944	0.0407/0.1005
^a $R_1 = \sum F_o - F_c / \sum F_o $, $wR_2 = \{ \sum w[(F_o)^2 - (F_c)^2]^2 / \sum w[(F_o)^2]^2 \}^{1/2}$			

Table S2. Bond lengths [Å] and angles [deg] for **LaL**.

La(1)-O(1)#1	2.458(5)	La(1)-O(4)#2	2.463(5)
La(1)-O(5)#3	2.509(5)	La(1)-O(2)#4	2.519(5)
La(1)-O(6)#5	2.525(5)	La(1)-O(5)#5	2.615(5)
La(1)-O(4)	2.631(5)	La(1)-O(1)#4	2.723(5)
O(1)#1-La(1)-O(4)#2	89.23(18)	O(1)#1-La(1)-O(5)#3	70.21(16)
O(4)#2-La(1)-O(5)#3	77.50(16)	O(1)#1-La(1)-O(2)#4	135.5(3)
O(4)#2-La(1)-O(2)#4	109.3(2)	O(5)#3-La(1)-O(2)#4	74.8(2)
O(1)#1-La(1)-O(6)#5	77.03(18)	O(4)#2-La(1)-O(6)#5	93.49(19)
O(5)#3-La(1)-O(6)#5	145.99(18)	O(2)#4-La(1)-O(6)#5	138.2(2)
O(1)#1-La(1)-O(5)#5	121.08(16)	O(4)#2-La(1)-O(5)#5	72.30(16)
O(5)#3-La(1)-O(5)#5	147.19(15)	O(2)#4-La(1)-O(5)#5	103.2(3)
O(6)#5-La(1)-O(5)#5	50.20(16)	O(1)#1-La(1)-O(4)	71.69(16)
O(4)#2-La(1)-O(4)	147.42(14)	O(5)#3-La(1)-O(4)	71.32(16)
O(2)#4-La(1)-O(4)	71.6(3)	O(6)#5-La(1)-O(4)	107.01(18)

O(5)#5-La(1)-O(4)	140.16(16)	O(1)#1-La(1)-O(1)#4	156.21(4)
O(4)#2-La(1)-O(1)#4	70.04(17)	O(5)#3-La(1)-O(1)#4	93.28(16)
O(2)#4-La(1)-O(1)#4	48.7(3)	O(6)#5-La(1)-O(1)#4	114.61(17)
O(5)#5-La(1)-O(1)#4	64.67(14)	O(4)-La(1)-O(1)#4	120.26(15)

Symmetry transformations used to generate equivalent atoms:

#1 $x+1/2, y+1/2, z$ #2 $-x+3/2, y+1/2, -z$ #3 $x, y+1, z-1$
 #4 $-x+1, y+1, -z$ #5 $-x+3/2, y+3/2, -z+1$

Table S3. Bond lengths [Å] and angles [deg] for **EuL**.

Eu(1)-O(8)#1	2.353(5)	Eu(1)-O(9)#2	2.354(6)
Eu(1)-O(7)#3	2.388(6)	Eu(1)-O(6)#4	2.401(5)
Eu(1)-O(10)#5	2.438(4)	Eu(1)-O(5)	2.436(5)
Eu(1)-O(8)#3	2.515(6)	Eu(1)-O(6)	2.516(5)
Eu(1)-O(9)#5	2.629(6)		
O(8)#1-Eu(1)-O(9)#2	89.1(2)	O(8)#1-Eu(1)-O(7)#3	156.9(2)
O(9)#2-Eu(1)-O(7)#3	105.9(2)	O(8)#1-Eu(1)-O(6)#4	78.58(18)
O(9)#2-Eu(1)-O(6)#4	69.53(18)	O(7)#3-Eu(1)-O(6)#4	122.74(19)
O(8)#1-Eu(1)-O(10)#5	109.0(2)	O(9)#2-Eu(1)-O(10)#5	134.7(3)
O(7)#3-Eu(1)-O(10)#5	72.9(2)	O(6)#4-Eu(1)-O(10)#5	73.9(2)
O(8)#1-Eu(1)-O(5)	94.5(2)	O(9)#2-Eu(1)-O(5)	74.49(19)
O(7)#3-Eu(1)-O(5)	73.5(2)	O(6)#4-Eu(1)-O(5)	143.38(19)
O(10)#5-Eu(1)-O(5)	140.7(2)	O(8)#1-Eu(1)-O(8)#3	149.45(16)
O(9)#2-Eu(1)-O(8)#3	72.76(19)	O(7)#3-Eu(1)-O(8)#3	53.57(18)
O(6)#4-Eu(1)-O(8)#3	72.18(18)	O(10)#5-Eu(1)-O(8)#3	71.4(3)
O(5)-Eu(1)-O(8)#3	103.62(19)	O(8)#1-Eu(1)-O(6)	72.95(18)
O(9)#2-Eu(1)-O(6)	120.61(17)	O(7)#3-Eu(1)-O(6)	84.26(19)
O(6)#4-Eu(1)-O(6)	149.23(17)	O(10)#5-Eu(1)-O(6)	104.5(3)
O(5)-Eu(1)-O(6)	52.20(17)	O(8)#3-Eu(1)-O(6)	137.43(17)
O(8)#1-Eu(1)-O(9)#5	70.69(18)	O(9)#2-Eu(1)-O(9)#5	157.59(6)
O(7)#3-Eu(1)-O(9)#5	96.3(2)	O(6)#4-Eu(1)-O(9)#5	96.27(17)
O(10)#5-Eu(1)-O(9)#5	49.8(3)	O(5)-Eu(1)-O(9)#5	115.49(18)
O(8)#3-Eu(1)-O(9)#5	120.57(17)	O(6)-Eu(1)-O(9)#5	63.57(16)

Symmetry transformations used to generate equivalent atoms:

#1 $x, y+1, z-1$ #2 $-x+1, y+1, -z+1$ #3 $-x+1/2, y+3/2, -z+1$
 #4 $-x+1/2, y+1/2, -z$ #5 $x-1/2, y+1/2, z-1$

Table S4. Bond lengths [Å] and angles [deg] for **TbL**.

Tb(1)-O(5)#1	2.334(4)	Tb(1)-O(9)#2	2.343(5)
Tb(1)-O(6)#3	2.370(5)	Tb(1)-O(8)#4	2.383(4)
Tb(1)-O(10)#5	2.408(4)	Tb(1)-O(7)	2.419(5)
Tb(1)-O(5)#3	2.490(5)	Tb(1)-O(8)	2.497(5)
Tb(1)-O(9)#5	2.638(5)		
<hr/>			
O(5)#1-Tb(1)-O(9)#2	89.20(18)	O(5)#1-Tb(1)-O(6)#3	156.27(17)
O(9)#2-Tb(1)-O(6)#3	106.96(19)	O(5)#1-Tb(1)-O(8)#4	78.62(16)
O(9)#2-Tb(1)-O(8)#4	69.72(16)	O(6)#3-Tb(1)-O(8)#4	122.87(17)
O(5)#1-Tb(1)-O(10)#5	108.5(2)	O(9)#2-Tb(1)-O(10)#5	134.9(3)
O(6)#3-Tb(1)-O(10)#5	72.4(2)	O(8)#4-Tb(1)-O(10)#5	73.7(2)
O(5)#1-Tb(1)-O(7)	94.93(19)	O(9)#2-Tb(1)-O(7)	73.71(17)
O(6)#3-Tb(1)-O(7)	73.9(2)	O(8)#4-Tb(1)-O(7)	142.89(17)
O(10)#5-Tb(1)-O(7)	141.2(2)	O(5)#1-Tb(1)-O(5)#3	149.85(14)
O(9)#2-Tb(1)-O(5)#3	73.07(16)	O(6)#3-Tb(1)-O(5)#3	53.78(15)
O(8)#4-Tb(1)-O(5)#3	72.47(16)	O(10)#5-Tb(1)-O(5)#3	71.5(3)
O(7)-Tb(1)-O(5)#3	102.87(17)	O(5)#1-Tb(1)-O(8)	73.16(16)
O(9)#2-Tb(1)-O(8)	120.10(15)	O(6)#3-Tb(1)-O(8)	83.59(16)
O(8)#4-Tb(1)-O(8)	149.63(15)	O(10)#5-Tb(1)-O(8)	104.8(3)
O(7)-Tb(1)-O(8)	52.46(15)	O(5)#3-Tb(1)-O(8)	136.81(14)
O(5)#1-Tb(1)-O(9)#5	70.47(16)	O(9)#2-Tb(1)-O(9)#5	157.83(6)
O(6)#3-Tb(1)-O(9)#5	95.11(18)	O(8)#4-Tb(1)-O(9)#5	96.80(15)
O(10)#5-Tb(1)-O(9)#5	50.1(3)	O(7)-Tb(1)-O(9)#5	115.60(16)
O(5)#3-Tb(1)-O(9)#5	120.81(15)	O(8)-Tb(1)-O(9)#5	63.43(14)

Symmetry transformations used to generate equivalent atoms:

#1 $x, y-1, z+1$ #2 $-x+1, y-1, -z+1$ #3 $-x+3/2, y-3/2, -z+1$

#4 $-x+3/2, y-1/2, -z+2$ #5 $x+1/2, y-1/2, z+1$

5. PXRD Analysis

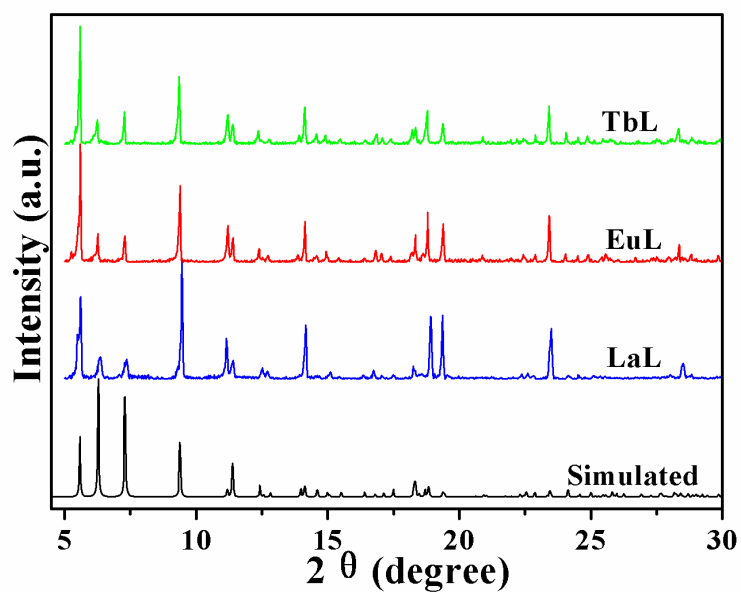


Fig. S1 Powder XRD patterns of compounds in the range from 5 to 30 degrees.

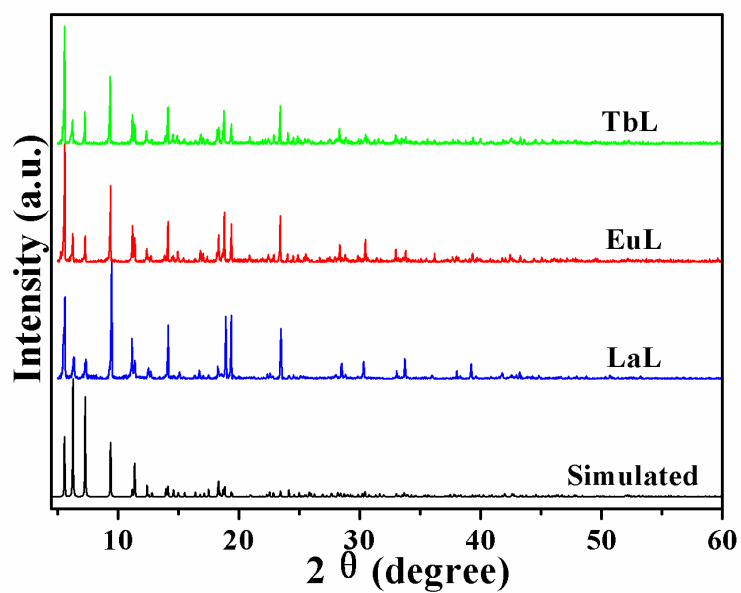


Fig. S2 Powder XRD patterns of compounds in the range from 5 to 60 degrees.

6. Luminescence measurements

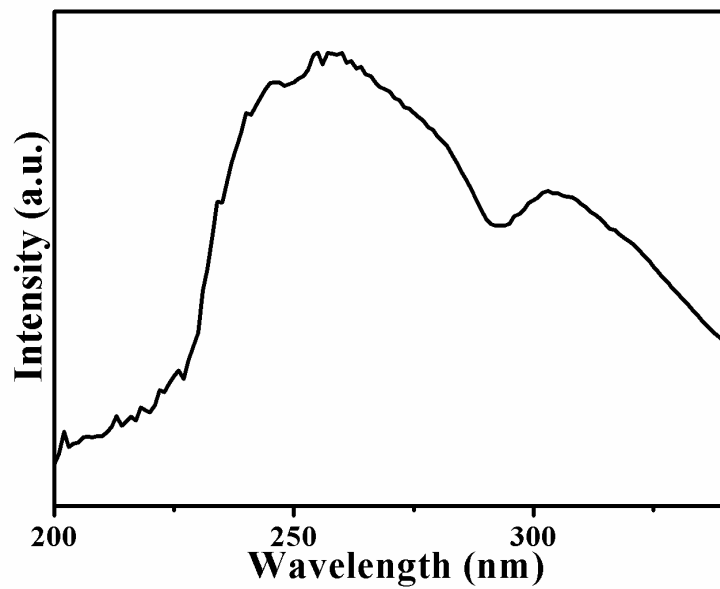


Fig. S3 Excitation (black, $\lambda_{em} = 612$ nm) of **EuL**.

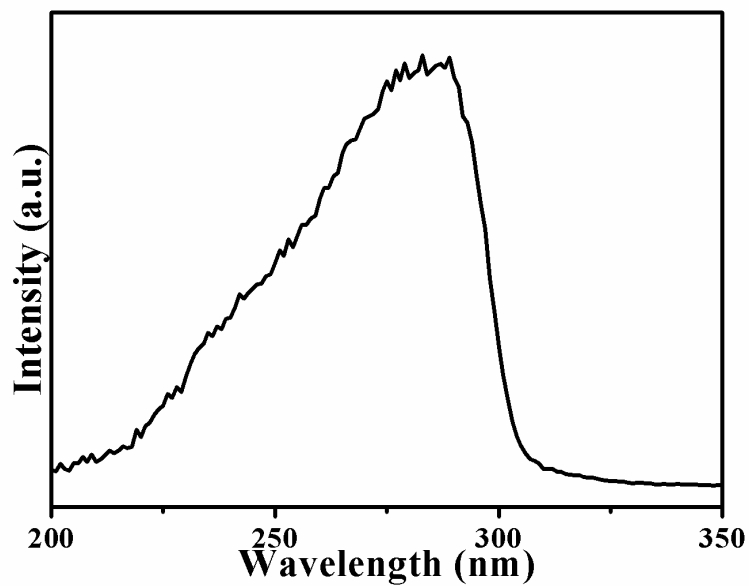


Fig. S4 Excitation (black, $\lambda_{em} = 544$ nm) of **TbL**.

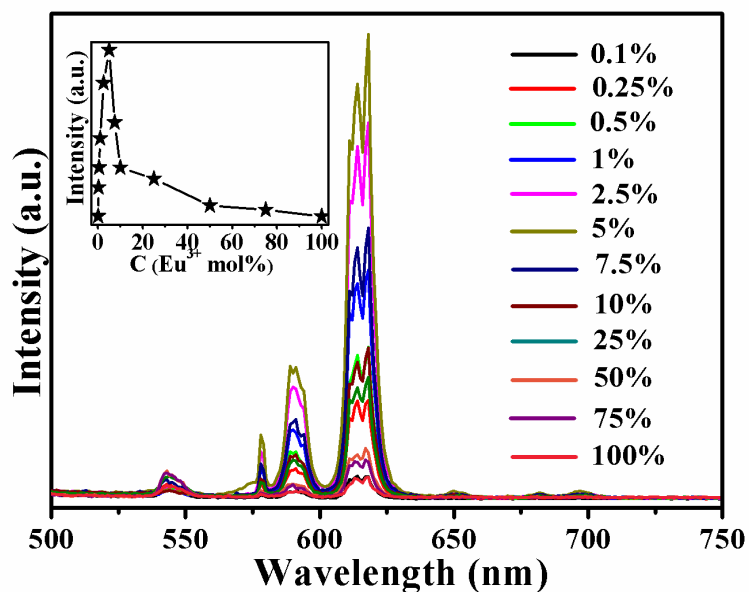


Fig. S5 PL emission spectra of Eu doped LaL, solid samples. The inset figures indicate corresponding transition intensities of doped samples as a factor of doping Eu^{3+} concentration.

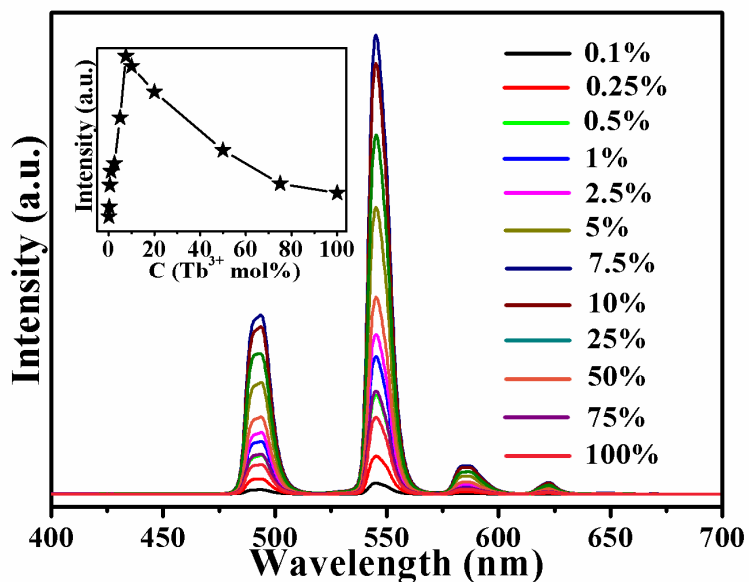


Fig. S6 PL emission spectra of Tb doped LaL, solid samples. The inset figures indicate corresponding transition intensities of doped samples as a factor of doping Tb^{3+} concentration.

7. Diffuse reflection spectra

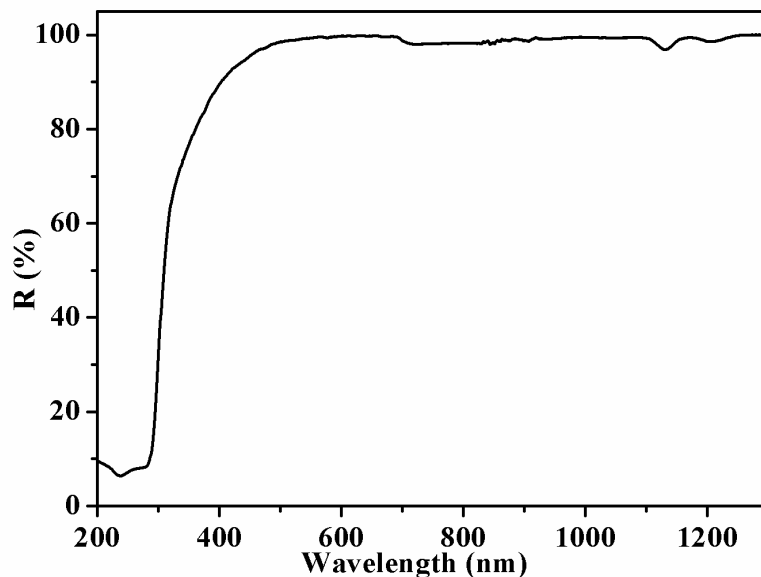


Fig. S7 Diffuse reflection spectra of **EuL**.

8. Thermogravimetric Analysis

The TGA analyses of **LnL** (Ln = La, Eu, Tb) were carried out, shown in Fig. S4. The TGA diagrams of the three compounds are quite similar, and all show two main weight losses in the curves. For **LaL**, the first weight loss of 13.59% is close to the calculated value (13.31%) corresponding to the loss of the DMF molecule in the range of 100 and 250 °C, and the second weight loss of 64.85% between 300 °C and 550 °C is attributed to the loss of ligand composite (calculated: 64.62%). The final residues are composed of La₂O₃. The weight loss of other **LnL** compounds (Ln = La, Eu, Tb) with the increase of temperature are similar to **LaL**, and all fits well with the calculated value.

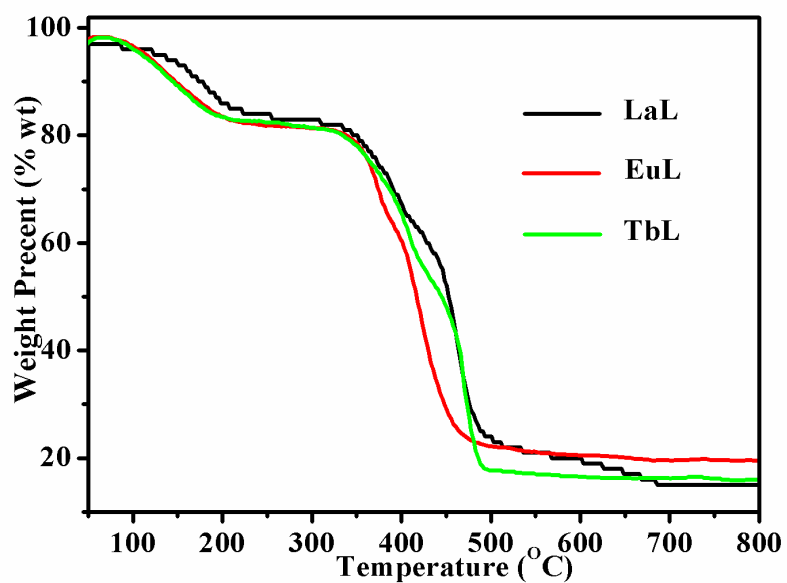


Fig. S8 Thermogravimetric analyses of **LnL** (Ln = La, Eu, Tb).

9. NLO measurements

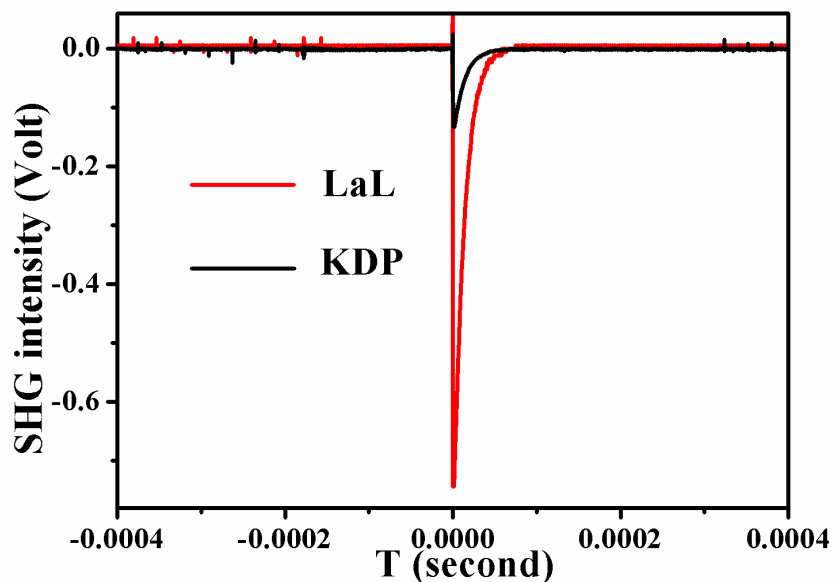


Fig. S9 Oscilloscope traces of the SHG signals of **LaL** and **KDP** at the same particle size of 150-210 μm .

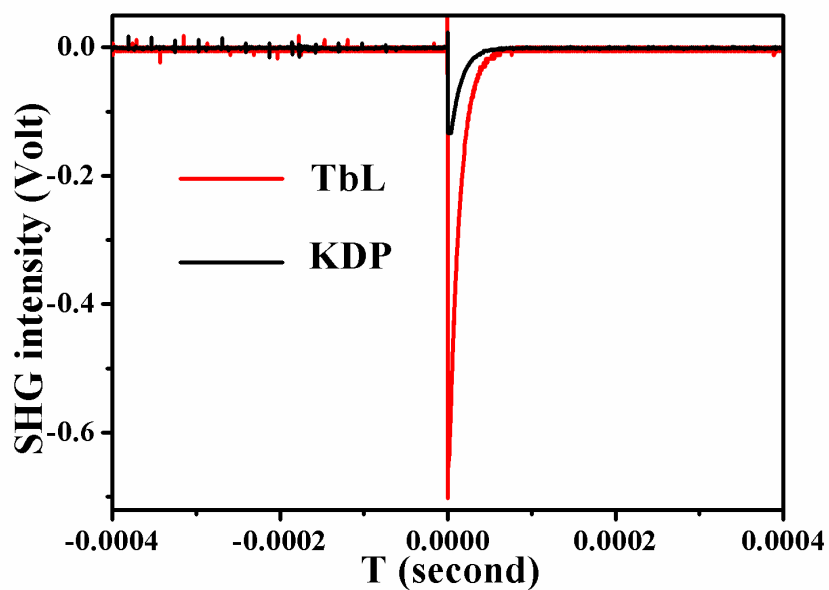


Fig. S10 Oscilloscope traces of the SHG signals of **TbL** and **KDP** at the same particle size of 150-210 μm .

References

- [1] H. Y. Wu, R. X. Wang, W. Yang, J. Chen, Z. M. Sun, J. Li, H. Zhang, *Inorg. Chem.* **2012**, *51*, 3103.